Influence of the oxidation state of $SrTiO_3$ plasmas for stoichiometric growth of pulsed laser deposition films identified by laser induced fluorescence

Kasper Orsel,[1,a] Rik Groenen,[2] Bert Bastiaens,[1] Gertjan Koster,[2] Guus Rijnders,[2] and Klaus-J. Boller[1]
[1]*Laser Physics and Nonlinear Optics, Department of Science and Technology, MESA+ Institute for Nanotechnology, University of Twente, Enschede, The Netherlands*
[2]*Inorganic Materials Science, Department of Science and Technology, MESA+ Institute for Nanotechnology, University of Twente, Enschede, The Netherlands*

(Received 10 July 2015; accepted 2 October 2015; published online 19 October 2015)

By applying two-dimensional laser induced fluorescence (LIF) on multiple plasma constituents, we are able to directly link the oxidation of plasma species in a $SrTiO_3$ plasma for pulsed laser deposition to the stoichiometry and quality of the thin films grown. With spatiotemporal LIF mapping of the plasma species in different background gas compositions, we find that Ti and Sr have to be fully oxidized for a stoichiometric growth of crystalline thin films, which gives new input for modeling surface growth, as well as provides additional control over the exact degree of stoichiometry of thin films. [http://dx.doi.org/10.1063/1.4933217]

Pulsed laser deposition (PLD) has been demonstrated to be a superior technique for the growth of thin films of complex crystalline oxides such as to impose ferroelectricity,[1] two-dimensional electron gases at heterointerfaces,[2] or superconductivity at interfaces,[3] among other applications.[4] It is widely accepted that PLD allows for stoichiometric transfer of complex materials, making it a very powerful and universal deposition technique.

However, the growing of stoichiometric and defect-free films is far from trivial. Deposition is the result of complex spatiotemporal, plasma-chemical dynamics. This renders the growth of films highly dependent on the external growth parameters, such as ablation laser fluence[5,6] and background gas pressure and composition,[7] in manners that are not well understood. More specifically, the often stringent requirements concerning the external parameters to grow high-quality defect-free films indicate that the state in which plasma constituents arrive at the substrate (oxidation state, propagation speed, and arrival time of different components) is of equal or even greater importance than just the stoichiometric transfer of materials. This can been seen, for instance, by the complex interplay between ablation fluence and target-substrate distance, and their combined influence on the thin film stoichiometry.[8]

Using spatially and temporally resolved spectroscopy that can yield distributions of constituents of the plasma allows us to trace dynamical processes, such as the generation and propagation of oxidation fronts. Especially in chemically reactive plasmas, a direct link to the exact molecular state in which material arrives at the substrate can be the key to a deeper understanding of growing perfect crystalline thin films as cannot be gained via blind optimization of PLD parameters, but is required for a future upscaling of crystalline growth to larger areas.

Of particular interest is to investigate film growth in a well-known and well-investigated PLD reference system, $SrTiO_3$ (STO) on a crystalline STO substrate. This allows sensitive X-ray diffraction measurements of the quality of growth, because even small defects in the film growth significantly change the lattice parameters.

[a]k.orsel@utwente.nl

Here, we investigate the stoichiometry of the film growth while systematically varying the chemical background gas composition, changing the mixture of O_2 and Ar, while maintaining the absolute total pressure constant. For an increasing fraction of O_2, we observe a transition from non-stoichiometric to stoichiometric film growth. Specifically, the film quality shows a distinct leap to perfectly stoichiometric STO, which occurs at a certain O_2 fraction (≈60%) of a total pressure of 0.1 mbar. A total background pressure of 0.1 mbar is chosen as the plasma expansion is no longer in the ballistic regime and has a strong interaction with the background gas, moderating the kinetic energy of the ablated species.[7] Argon and oxygen have a similar atomic weight and PLD plasmas exhibit very similar expansion dynamics in either Ar or O_2.[9] By mixing Ar and O_2, we maintain a constant total pressure in all measurements with comparable gas dynamic processes, such as expansion, propagation speed, and collision rates, for all gas mixtures. As the ablation laser fluence is kept constant for all measurements, changes in plasma composition will be primarily caused by a change in chemical processes and not by changing dynamics.

By comparison with optically recorded TiO and SrO spatiotemporal distributions in the plasma, we find that the oxidation state of Ti and Sr upon arrival at the substrate is correlated with the stoichiometry of growth. The optical measurements show that all Ti needs to be oxidized at the substrate location for achieving stoichiometric growth. Based on the SrO measurements, we conclude that this is also the case for Sr. These results provide a direct link and thus predictability for controlling the chemical plasma composition and subsequent growth of complex oxide thin films.

The spatiotemporal mapping of the plasma constituents is carried out in a custom built PLD chamber, a detailed description of which can be found in a previous article of ours.[10] We use laser induced fluorescence (LIF) instead of the more commonly used optical emission spectroscopy (OES),[7,11,12] because OES is limited to the detection of excited particles that happen to spontaneously fluoresce. Another disadvantage of OES is that the excited state populations are orders of magnitude lower than the ground state populations when the plume has expanded close to the substrate.[13] In contrast, LIF enables us to excite and detect ground state species at freely selectable locations and times and in a chemically specific manner. This is of particular importance when selecting long delay times with respect to the moment of ablation, when the plume has cooled down and expanded over typically several centimeters towards the substrate.[14–16]

Target ablation is done with laser pulses generated by a KrF excimer laser (248 nm, 30 ns duration FWHM, operating at 2 Hz). A mask, placed in the KrF laser beam to select a spatially uniform beam, is imaged onto the target, resulting in a laser spot of 0.91×2.42 mm^2. Through control of the laser output energy, the laser fluence is kept at $1.3 \pm 10\%$ J/cm^2 during all measurements. The UV excitation wavelengths for LIF in the range from 250 to 350 nm are generated by frequency doubling the output of a dye laser pumped with the second harmonic (532 nm) output of a Q-switched Nd:YAG laser (7 ns FWHM). The UV output, which has a pulse duration of 4 ns FWHM, a bandwidth of 8.1 pm and 75 μJ per pulse, is transformed into a thin sheet in the plane of the forward propagation of the plasma plume from the ablation spot on the target to the center of the substrate. The sheet has an in-plane focus of approximately 0.4 mm thickness.

To image the neutral titanium distribution in the plasma plume, we use a transition from the atomic ground state ($3d^2 4s^2\ a^3F$) to the $3d^2(^1G)4s4p(^3P^\circ)v^3F^\circ$ state at 294.1995 nm. Relaxation occurs to the $3d^3(^4F)4sb^3F$ state via fluorescence at 445.3313 nm.[17] A narrowband interference filter with a bandpass of 437–447 nm transmits the LIF of Ti while suppressing the thermally induced spontaneous emission (SE) of the plasma. The excitation of titanium oxide is done using an $X^3\Delta \rightarrow D$ transition at 301.47 nm and detecting the red-shifted LIF between 301 and 310 nm.[18] Strontium oxide is excited using an $X^1\Sigma \rightarrow C^1\Sigma$ transition at 350.38 nm and detected using the red-shifted LIF from relaxation to various different rotational and vibrational states of $X^1\Sigma$.[18] For both TiO and SrO, the SE of the plasma is suppressed by a colored glass band-pass filter transmitting 275–375 nm. A background subtraction using measurements with the LIF beam blocked is applied to all LIF measurements to remove any residual SE from the plasma that is transmitted by the band-pass filters. To reduce the influence of shot-to-shot fluctuations, all measurements are averaged over 30 shots. To improve the quality of the spatiotemporal mapping measurements, we decided to carry these out with the substrate removed, because in our setup with an oblique angle of the LIF beam, the substrate caused unwanted optical reflections. This modification avoids artifacts

for the relevant observation times, until the plume arrives at the location of the substrate. The films deposited for the XRD measurements are grown on a substrate heated to 710 °C. The influence of substrate heating on the propagation dynamics of the plasma plume,[19] present during deposition but absent during LIF measurements, is largely avoided by using laser substrate heating instead of the more commonly used resistive substrate heating. We performed comparative measurements of plume propagation with either a laser heated target at 710 °C or at room temperature,[20] which showed little difference, demonstrating the validity of the LIF measurements without heated substrate. In contrast, plume propagation with a resistive heated substrate at 710 °C showed, compared to room temperature, large changes in propagation similar as described by Sambri *et al.*[19]

To investigate the chemical composition of the plasma plume and, more specifically, the effects of the background gas composition on the oxidation of the plasma constituents, we attempted to map the spatio-temporal distribution of all relevant and expectantly dominant plasma constituents which are Ti, TiO, TiO_2, Sr, and SrO. The location, density, and arrival time of these species is mapped in a background gas of which the total pressure is held constant at 0.1 mbar. The partial pressure of O_2 is step-wise increased from 0% to 100% in order to step-wise increase the chemical reactivity.

The LIF signal of strontium atoms excited at either 293.18 and 689.25 nm could be detected, unfortunately, only close to the noise level and only at small delay times (<10 μs) in pure Ar. Excitation at 460.73 nm might yield a higher fluorescence signal. However, generating this wavelength is not possible with our current setup. Similarly, measuring TiO_2 densities proved difficult with excitation lines at 562.56 nm and 556.67 nm as described by Zhuang *et al.*,[21] due to strong background noise from scattering of the LIF laser, when using the LIF laser in the visible range.

To be able to relate the LIF signal to the material density, all excitation transitions used are driven into saturation. In saturation, a variation in laser power, for example, pulse-to-pulse fluctuations or spatial inhomogeneities, will not result in variations of the LIF signal. Thereby, the LIF signal becomes proportional to the density of the excited species. However, since the measurements are not calibrated on an absolute scale, the density of one species cannot be absolutely compared to that of another species.

Figure 1 shows typical results of distribution measurements for a cross-section of the plasma plume in the propagation plane from the target (z = x = 0 mm) to where the substrate is positioned during growth experiments (x = 0 mm, z ≈ 50 mm). Two images of half of the plasma plume are shown next to each other for easier comparison. Figure 1(a) shows the Ti distribution on the left and the TiO distribution on the right as recorded with the 0.1 mbar background consisting of 100% O_2 gas, at 20 μs delay after ablation, when the front of the plume has not yet reached the substrate

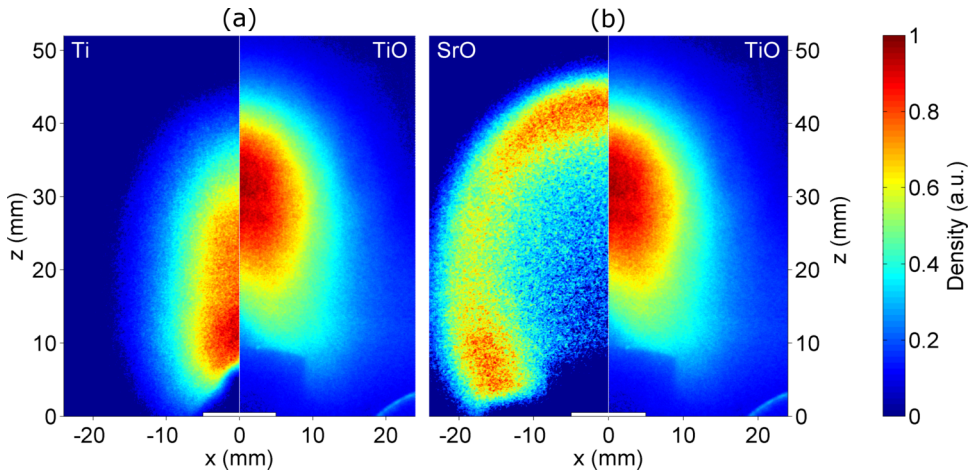

FIG. 1. Normalized density distributions of several components of a STO plasma plume cross-section in the propagation plane from the target (z = x = 0 mm) to the center of the substrate position (x = 0 mm, z = 50 mm). The lhs of (a) displays the Ti ground state density and the rhs displays TiO. In (b), respectively, SrO and TiO are displayed. The densities shown are measured at 20 μs delay after ablation and obtained with 0.1 mbar pure O_2 as background gas. The lack of signal close to the center of the target (x = 0, z = 0) is caused by the target holder obscuring one edge of the LIF excitation beam.

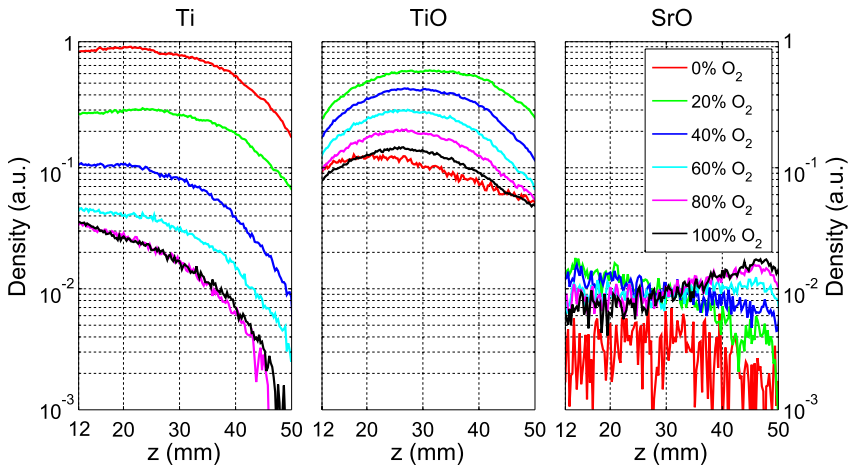

FIG. 2. The ground state population densities of Ti, TiO, and SrO measured along the propagation axis, z (x = 0), at different partial pressures of O_2. All measurements are done at a delay of 35 μs from target ablation and in 0.1 mbar total background pressure. The first 12 mm is not shown as it is obstructed by the target holder.

region (around z = 50 mm). Figure 1(b) shows the distribution of SrO (left) next to TiO (right) under the same conditions. These measurements display a strong spatial separation of the different plasma species. It can be seen that SrO is located primarily in the outer most edges of the plume, whereas TiO is largely absent from the plasma edges and is concentrated in the center of the plume. Neutral titanium is found to be confined even more to the center, as well as close to the target.

In Fig. 2 are shown the ground state population densities of Ti, TiO, and SrO along the propagation axis (at x = 0 mm in Fig. 1) as function of the distance from the target, z, at different partial pressures of O_2. The densities and oxidation state of plasma species along the propagation axis are of particular interest, especially close to the substrate location, as this displays the material that arrives at the center of the substrate, the location where growth is typically being optimized. Species further away from the propagation axis will either deposit on the outer ranges or edges of the substrate or even disappear into the PLD chamber. These measurements are taken for a delay of 35 μs between ablation and detection, at which time the plasma plume has expanded to the substrate location, which is typically located 50 mm from the target. To emphasize the strong differences in spatial changes of densities, all densities are normalized to the maximum of the Ti, which itself is normalized to unity. Since our approach monitors the relative spatiotemporal distribution for the various species, the ratio in absolute data between different species reflects their ratio in fluorescence yield. The SrO density determined as described above is close to our detection limit (10^{-3} in Fig. 2), because the LIF signal is only about a factor of ten above the background noise when no O_2 is supplied (100% Ar). The noise is caused by residual spontaneous emission of the plasma that is not removed by the background subtraction. In the Ti distribution, a remarkable drop by almost two orders of magnitude can be seen for all distances from the target when the oxygen fraction is increased but is less than 80%. At 80% and above (which is pure O_2), the Ti density does not decrease and the distribution does not change anymore. In other words, the Ti distribution along the z-axis retracts away from the substrate position (z = 50 mm) with increasing O_2 fraction. The on-axis TiO density distribution is low when no O_2 is supplied (lowest trace). The highest TiO concentration, at all z-values, is seen with 20% O_2, and decreases moderately with increasing O_2 fraction, while the shape of the TiO distribution does not change much except for an overall factor. Another observation is that the density distribution in pure O_2 is actually very similar to the case when no O_2 is supplied at all (pure Ar). The SrO distribution shows an increase by almost an order of magnitude in density in the front of the expanding plume with increasing O_2 fractions, while the density closer to the target slightly decreases. Similar to Ti, the distributions at 80% and 100% O_2 are nearly identical.

In Fig. 3 we show the total amount of Ti, TiO, and SrO present in the plume as function of delay time from target ablation for different partial pressures of O_2. This plot allows to identify the chemical processes taking place in the entire plasma plume, and specifically, to separate the influence

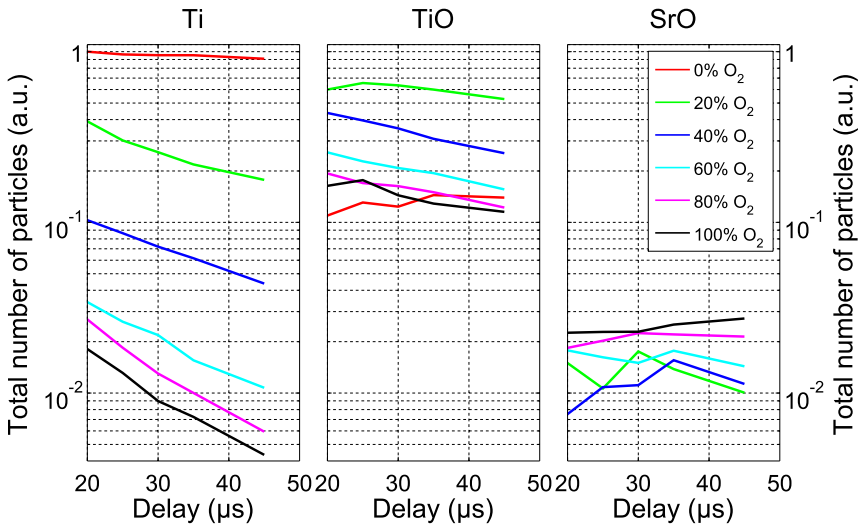

FIG. 3. Total amount of Ti, TiO, and SrO in the plasma plume, acquired by spatially integrating the LIF signal over the entire plume as function of the delay with respect to the moment of target ablation, for different partial pressures of O_2. All measurements are at 0.1 mbar total background pressure. In the first 20 μs, a significant part of the plasma plume is obscured by the target holder and therefore not accessible for LIF measurements.

of the oxygen that is inherently present in the plasma plume, supplied by the target, and the oxygen that is supplied by the background gas. The total number of particles shown in Figure 3 is acquired by spatially integrating the LIF signal for Ti, TiO, and SrO over the entire plasma plume, taking the cylindrical symmetry around the z-axis (x = y = 0) into account. Similar to the density distribution in Figure 2, all plots of the particle numbers are normalized to the maximum number of particles of Ti, which itself is normalized to unity. The first 20 μs are not shown, as part of the plasma plume close to the target is obscured by the target holder and therefore not accessible for LIF measurements. Similar to the density distributions, Ti shows the most prominent change with increasing oxygen fraction. Without any O_2 supplied, the total amount of Ti atoms is nearly constant in time, whereas the Ti amount decreases strongly, by almost two orders of magnitude, when the oxygen fraction is increased. With O_2 present, the amount of Ti decreases vs. time, with a steepening slope the more O_2 is present. In comparison, a large increase in total amount of TiO is visible when a small amount of oxygen is added, but the amount of TiO decreases again with higher O_2 fractions, returning to values in pure O_2 that are almost identical to those without O_2. As function of delay time, the low amount of TiO particles is almost constant in a pure argon background, turning into a weak decrease vs. time with increasing oxygen fraction. The total number of SrO molecules as function of the oxygen fraction in the background gas shows only a small increase. Also, as function of delay time, the number of SrO particles remains almost constant for all oxygen fractions. The strong fluctuations in amount over time are caused by the large amount of noise present close to the detection limit.

Our physical interpretation of the spatiotemporal data in Figs. 2 and 3 is that a strong mixing of the background gas into the plasma plume takes place, facilitating the oxidation of Ti to TiO and of TiO to TiO_2. Both plots show that both the density and amount of titanium steadily decrease with an increasing oxygen fraction in the background gas. Strong mixing of the background gas and plasma plume has been previously concluded by Sasaki and Watarai.[22]

At higher levels of oxygen (80% and 100% O_2), it can be seen that no significant amount of neutral Ti reaches the substrate location. Density distributions at longer delay times even show the front of Ti retracting towards the target. In comparison, the total amount of Ti in pure Ar remains almost the same over time, indicating that little to no oxidation takes place in the plasma plume with oxygen released from the target. This shows that it is the O_2 from the background gas that is responsible for fully oxidizing the plasma species. Interestingly, very little difference is visible between the Ti densities at 80% and 100% oxygen, indicating that above a certain threshold, somewhere between 60% and 80%, the amount of available oxygen no longer is the bottleneck for oxidation of Ti.

The described reaction dynamics are confirmed when inspecting the next species in the oxidation of Ti, TiO, and TiO_2, which is the TiO concentration. Our measurements show that the density of TiO strongly increases when a small amount of oxygen (20%) is added to the background gas, but steadily decreases again when the percentage of oxygen is increased further. We conclude that the latter decrease is caused by further oxidation of TiO to TiO_2, because TiO is an intermediate between Ti and TiO_2 and the Ti density continuously decreases with an increasing O_2 fraction, although the TiO_2 molecular fluorescence signal turned out to be too weak for detection with our setup.

No SrO is detected in the plasma when ablating in pure argon, or at least only present in small quantities. The density measurement in pure Ar yielded signals of the same strength as the noise, as shown in Figure 2, making these measurements less reliable. Nevertheless, the lack of SrO in pure Ar and the relatively small increase of the amount of SrO with O_2 increasing from 20% to 100% suggests that Sr oxidizes strongly and only requires little O_2 to fully oxidize. This is supported by the observation that adding a small amount of oxygen in the background gas lets SrO appear in the center of the plasma plume. When increasing the oxygen fraction, an increasing amount of SrO is formed on the front edge of the plasma plume (Figure 2), where interaction with the background gas is strongest. A small decrease in SrO amount is visible near the center of the plume. A possible explanation for this behavior is that the reaction $Sr + O_2 \rightleftarrows SrO + O$ is strongly dependent on temperature and relative concentration of the four products.[23] As the O concentration inside the plume will increase due to reactions of Ti and TiO with O_2, the reaction $SrO + O \rightarrow Sr + O_2$ could become more common, leading to a decrease in SrO concentration in the plume center.

The spatiotemporal mapping measurements of Ti, TiO, and SrO show a significant change in plasma composition of the plume, especially in the front edge of the plume, when it reaches the substrate. To be able to link these plasma composition measurements directly to the thin film growth, we have grown STO films on STO under the same conditions (varying the Ar/O_2 mixture at constant pressure), with the substrate at z = 50 mm, for a subsequent analysis with X-ray diffraction (XRD). The LIF and XRD measurements are done at slightly different absolute pressures, 0.1 and 0.08 mbar, respectively. However, we verified that this small difference does not have a noticeable effect on our results, based on XRD and LIF comparisons of 100% O_2 at 0.08 mbar vs. 80% O_2 at 0.1 mbar. Figure 4 shows symmetrical XRD scans around the (002) Bragg reflection of $SrTiO_3$ for these thin films. The film grown in 0% oxygen (pure Ar) shows a clear film peak, as indicated by the arrow, aside from the strong substrate peak at 46.5°. This indicates an increased lattice parameter

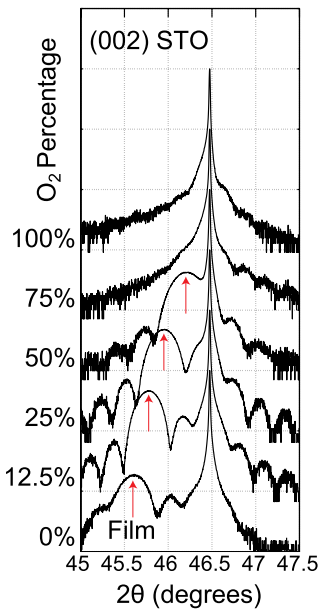

FIG. 4. XRD scans around the (002) Bragg reflection of STO. It shows scans of samples grown at partial oxygen pressures and a total pressure of $8 \cdot 10^{-2}$ mbar.

with respect to the substrate.[24] This typically arises from cation defects in the lattice, increasing the volume of the unit cell. For homoepitaxially grown films, the increased volume results in an expansion of the c-axis, since these films are in-plane strained with regard to the $SrTiO_3$ substrate. With increasing O_2 fraction, the film peak moves closer to the substrate peak, indicating an improvement in stoichiometry.

A remarkable transition can be seen with further increased oxygen pressure (75% and above), in that the film peak vanishes. This proves that a significant increase in film quality takes place at a certain oxygen pressure, here at about 75%, where a clear transition takes place from non-stoichiometric to stoichiometric film growth.

At this point, we note that a sharp transition to high-quality growth within a narrow range of certain parameter settings is a well-known heuristic observation in PLD. A possible mechanism contributing to the change in stoichiometry might be the effect of preferential scattering, as described by Wicklein *et al.*[8] This effect implies that lighter plasma species scatter stronger than heavier species. In the case of STO, where Ti is significantly lighter than Sr, the plasma plume would be Sr rich when it reaches the substrate. However, oxidation of the plasma species increases their mass. Whereas the weight ratio for Sr/Ti is 1.8, for the oxidized species (SrO/TiO_2) it is only 1.3, reducing the effects of preferential scattering. In this paper, we present independent spatiotemporal mapping data of the species in the plasma plume that are responsible for the growth. In fact, when comparing the spectroscopic data with the structural data of the grown material, we find an important correlation: the transition from non-stoichiometric to stoichiometric growth in the XRD measurements coincides with an oxygen pressure where neutral atomic titanium ceases to reach the substrate, while both Ti and Sr reach the substrate in their fully oxidized state, which are, respectively, TiO_2 and SrO. Furthermore, the decrease of non-stoichiometry aligns with the decrease of Ti and with the increase of oxidized species. This strongly suggests that full oxidation of plasma constituents is clearly a necessary requirement for stoichiometric growth of STO.

To summarize, we have mapped dynamic oxidation processes of plasma species in the PLD process and have shown the strong influence of the composition of the background gas on the plasma plume composition. Comparing these spectroscopic data with X-ray diffraction data of the grown material quality, we find a clear correlation between the chemical composition of the leading edge of the plasma plume and the stoichiometry of the grown film. Above a specific O_2 fraction of the background gas, approximately 75%, when full oxidation of Ti and Sr in the leading edge of the plasma plume is reached, the film growth transides from non-stoichiometric to stoichiometric growth, as determined with X-Ray diffraction. This suggests that the oxidation of species of the plasma is a crucial mechanism in the stoichiometric reconstruction of the synthesized oxide thin films.

To illustrate how our findings may be applied in scaling stoichiometric PLD growth, one may consider the following example. If the target-substrate distance is decreased from 50 mm to 40 mm, while maintaining all other parameter settings, this would prohibit stoichiometric film growth, even in pure O_2, as Figure 2 shows that the oxidation of Ti would not be complete. Similarly, an increase in target-substrate distance would allow for stoichiometric growth in lower oxygen fractions than 75%, as the oxidation is allowed to progress further. Other examples and according spatiotemporal mapping can be devised for transversely upscaling PLD, for increasing the area of stoichiometric growth.

This research is supported by the Dutch Technology Foundation STW, which is part of the Netherlands Organization for Scientific Research (NWO) and partly funded by the Ministry of Economic Affairs (Project No. 10760).

[1] E. Bousquet, M. Dawber, N. Stucki, C. Lichtensteiger, P. Hermet, S. Gariglio, J. Triscone, and P. Ghosez, "Improper ferroelectricity in perovskite oxide artificial superlattices," Nature **452**, 732 (2008).
[2] A. Ohtomo and H. Hwang, "A high-mobility electron gas at the $LaAlO_3/SrTiO_3$ heterointerface," Nature **427**, 6973 (2004).
[3] N. Reyren, S. Thiel, A. Caviglia, L. F. Kourkoutis, G. Hammerl, C. Richter, C. Schneider, T. Kopp, A.-S. Rüetschi, D. Jaccard, M. Gabay, D. A. Muller, J.-M. Triscone, and J. Mannhart, "Superconducting interfaces between insulating oxides," Science **317**, 1196 (2007).
[4] *Pulsed Laser Deposition of Thin Films*, edited by R. Eason (John Wiley & Sons, Inc., 2007).
[5] T. Ohnishi, M. Lippmaa, T. Yamamoto, S. Meguro, and H. Koinuma, "Improved stoichiometry and misfit control in perovskite thin film formation at a critical fluence by pulsed laser deposition," Appl. Phys. Lett. **87**, 241919 (2005).

[6] C. Xu, S. Wicklein, A. Sambri, S. Amoruso, M. Moors, and R. Dittmann, "Impact of the interplay between nonstoichiometry and kinetic energy of the plume species on the growth mode of $SrTiO_3$ thin films," J. Phys. D: Appl. Phys. **47**, 034009 (2014).
[7] S. Amoruso, C. Aruta, P. Aurino, R. Bruzzese, X. Wang, F. M. Granozio, and U. S. di Uccio, "Oxygen background gas influence on pulsed laser deposition process of $LaAlO_3$ and $LaGaO_3$," Appl. Surf. Sci. **258**, 9116 (2012).
[8] S. Wicklein, A. Sambri, S. Amoruso, X. Wang, R. Bruzzese, A. Koehl, and R. Dittmann, "Pulsed laser ablation of complex oxides: The role of congruent ablation and preferential scattering for the film stoichiometry," Appl. Phys. Lett. **101**, 131601 (2012).
[9] S. Amoruso, B. Toftmann, and J. Schou, "Thermalization of a UV laser ablation plume in a background gas: From a directed to a diffusionlike flow," Phys. Rev. E **69**, 056403 (2004).
[10] K. Orsel, R. Groenen, H. Bastiaens, G. Koster, G. Rijnders, and K.-J. Boller, "Spatial and temporal mapping of Al and AlO during oxidation in pulsed laser ablation of $LaAlO_3$," J. Instrum. **8**, C10021 (2013).
[11] C. Aruta, S. Amoruso, R. Bruzzese, X. Wang, D. Maccariello, F. M. Granozio, and U. S. di Uccio, "Pulsed laser deposition of $SrTiO_3/LaGaO_3$ and $SrTiO_3/LaAlO_3$: Plasma plume effects," Appl. Phys. Lett. **97**, 252105 (2010).
[12] A. Sambri, D. Cristensen, F. Trier, Y. Chen, S. Amoruso, N. Pryds, R. Bruzzese, and X. Wang, "Plasma plume effects on the conductivity of amorphous-$LaAlO_3/SrTiO_3$ interfaces grown by pulsed laser deposition in O_2 and Ar," Appl. Phys. Lett. **100**, 231605 (2012).
[13] H. Döbele, T. Mosbach, K. Niemi, and V. S. von der Gathen, "Laser-induced fluorescence measurements of absolute atomic densities: Concepts and limitations," Plasma Sources Sci. Technol. **14**, S31 (2005).
[14] T. Okada and M. Maeda, "Laser spectroscopic studies of pulsed-laser deposition process for high-T_c thin films," Mater. Sci. Eng., B **47**, 64 (1997).
[15] C. Dutouquet and J. Hermann, "Laser-induced fluorescence probing during pulsed-laser ablation for three-dimensional number density mapping of plasma species," J. Phys. D: Appl. Phys. **34**, 3356–3363 (2001).
[16] Y. Nakata, T. Okada, M. Maeda, S. Higuchib, and K. Ueda, "Effect of oxidation dynamics on the film characteristics of Ce:YIG thin films deposited by pulsed-laser deposition," Opt. Lasers Eng. **44**, 147 (2006).
[17] A. Kramida, Y. Ralchenko, J. Reader, and NIST ASD Team, NIST atomic spectra database (version 5.1), 2013.
[18] R. Pearse and A. Gaydon, *The Identification of Molecular Spectra*, 3rd ed. (Chapman and Hall, London, 1976).
[19] A. Sambri, S. Amoruso, X. Wang, M. Radovic, F. M. Granozio, and R. Bruzzese, "Substrate heating influence on plume propagation during pulsed laser deposition of complex oxides," Appl. Phys. Lett. **91**, 151501 (2007).
[20] R. Groenen, "Understanding thin film growth in pulsed laser deposition; plasma plume chemistry" (unpublished).
[21] X. Zhuang, A. Le, T. C. Steimle, R. Nagarajan, V. Gupta, and J. P. Maier, "Visible spectrum of titanium dioxide," Phys. Chem. Chem. Phys. **12**, 15018 (2010).
[22] K. Sasaki and H. Watarai, "Dynamics of laser-ablation plume and ambient gas visualized by laser-induced fluorescence imaging spectroscopy," Jpn. J. Appl. Phys., Part 2 **45**, L447 (2006).
[23] C. Batalli-Cosmovici and K.-W. Michel, "Molecular beam study on BaO and SrO formation for clarifying interaction of meta-vapors with upper atmosphere oxygen," Planet. Space Sci. **21**, 89 (1972).
[24] B. Jalan, P. Moetakef, and S. Stemmer, "Molecular beam epitaxy of $SrTiO_3$ with a growth window," Appl. Phys. Lett. **95**, 032906 (2009).